Computers and Fluids 131 (2016) 151–168

Contents lists available at ScienceDirect

Computers and Fluids

journal homepage: www.elsevier.com/locate/compfluid

High-order fluid solver based on a combined compact integrated RBF approximation and its fluid structure interaction applications

C.M.T. Tien, D. Ngo-Cong, N. Mai-Duy, C.-D. Tran, T. Tran-Cong*

Computational Engineering and Science Research Centre, Faculty of Health, Engineering and Sciences, The University of Southern Queensland, Toowoomba, Queensland 4350, Australia

ARTICLE INFO

Article history:
Received 6 November 2015
Revised 17 March 2016
Accepted 17 March 2016
Available online 19 March 2016

Keywords:
Combined compact integrated RBF
Convection-diffusion equations
Fluid flow
Fluid structure interaction
Enclosed membrane
Immersed boundary

ABSTRACT

In this study, we present a high-order numerical method based on a combined compact integrated RBF (IRBF) approximation for viscous flow and fluid structure interaction (FSI) problems. In the method, the fluid variables are locally approximated by using the combined compact IRBF, and the incompressible Navier-Stokes equations are solved by using the velocity-pressure formulation in a direct fully coupled approach. The fluid solver is verified through various problems including heat, Burgers, convection-diffusion equations, Taylor-Green vortex and lid driven cavity flows. It is then applied to simulate some FSI problems in which an elastic structure is immersed in a viscous incompressible fluid. For FSI simulations, we employ the immersed boundary framework using a regular Eulerian computational grid for the fluid mechanics together with a Lagrangian representation of the immersed boundary. For the immersed fibre/membrane FSI problems, although the order of accuracy of the present scheme is generally similar to FDM approaches reported in the literature, the present approach is nonetheless more accurate than FDM approaches at comparable grid spacings. The numerical results obtained by the present scheme are highly accurate or in good agreement with those reported in earlier studies of the same problems.

1. Introduction

Although many scientific and engineering problems involve fluid structure interaction (FSI), thorough study of such problems remains a challenge due to their strong nonlinearity and multidisciplinary requirements [1–3]. For most FSI problems, closed form analytic methods to the model equations are often not available, while laboratory experiments are not practical due to limited resources. Therefore, to investigate the fundamental physics involved in the complicated interaction between fluids and solids, one has to rely on numerical methods [4].

In this study, we are interested in the interaction of a viscous incompressible fluid with an immersed elastic membrane. The immersed boundary method (IBM), originally developed by Peskin [5], is designed to solve this kind of problem. The IBM is a mixed Eulerian-Lagrangian scheme in which the fluid dynamics based on the Navier-Stokes (N-S) equations are described in Eulerian form, and the elasticity of the structure is described in Lagrangian form. The IBM considers the structure as an immersed boundary which can be represented by a singular force in the N-S equations rather than a real body. It avoids grid-conforming difficulties associated with the moving boundary faced by conventional body-fitted methods. The fluid computation is done on a fixed, uniform computational lattice and the representation of the immersed boundary is independent of this lattice. The immersed boundary exerts a singular force on the nearby lattice points of the fluid with the help of a computational model of the Dirac δ-function. At the same time, the representative material points of the immersed boundary move at the local fluid velocity, which is obtained by interpolation from the nearby lattice points of the fluid. The same δ-function weights are used in the interpolation step as in the application of the boundary forces on the fluid. Computer simulations using the IBM such as blood flow in the heart [5,6], insect flight [7], aquatic animal locomotion [8], bio-film processing [9], and flow past a pick-up truck [10] have exhibited the great potential of the IBM in FSI applications. Reviews on immersed methods can be found in [11,12].

High-order approximation schemes have the ability to produce highly accurate solutions to incompressible viscous flow problems. With these schemes, a high level of accuracy can be achieved using a relatively coarse discretisation. Many types of high-order approximation methods have been reported in the literature. Botella and Peyret [13] developed a Chebyshev collocation method for the lid-driven cavity flow. Various types of high-order compact finite difference algorithms (HOC) were proposed [14–16]. On the other

* Corresponding author. Tel.: +61746311332; fax: +61746312110.
E-mail address: thanh.tran-cong@usq.edu.au (T. Tran-Cong).

http://dx.doi.org/10.1016/j.compfluid.2016.03.021
0045-7930/

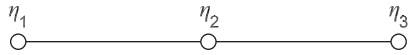

Fig. 1. Compact 3-point 1D-IRBF stencil for interior nodes.

hand, radial basis function networks (RBF) have emerged as a powerful approximation tool [17–19]. Different schemes of integrated RBF approximation (here referred to as IRBF) were developed in the literature [20–23]. In [24], the authors developed a high-order fully coupled scheme based on compact IRBF approximations for viscous flow problems, where nodal first- and second-derivative values are included in the stencil approximation and the starting points in the integration process are second-order derivatives. In their work, the N-S governing equations are taken in the primitive form where the velocity and pressure fields are solved in a direct fully coupled approach. With relatively coarse meshes, the compact IRBF produces very accurate solutions to many fluid flow problems in comparison with some other methods such as the standard central finite different method (FDM) and HOC. Recently, Tien et al. [25] proposed a combined compact IRBF approximation scheme, where nodal first- and second-derivative values are also included in the stencil approximation, but the starting points are fourth-order derivatives. The fourth-order IRBF approach allows a more straightforward incorporation of nodal values of first- and second-order derivatives, and yields better accuracy over previous IRBF approximation schemes.

In this paper, we will incorporate the high-order combined compact IRBF approximation introduced in [25] into the fully coupled N-S approach reported in [24]. The new high-order fluid solver is verified through various problems such as heat, Burgers, convection-diffusion equations, Taylor-Green vortex and lid driven cavity flows. It will show that highly accurate results are obtained with the present approach. Then, we embed the fluid solver in the IBM procedure outlined in [26,27] to simulate FSI problems in which a stretched elastic fibre/membrane relaxes in a viscous fluid. Comparisons between the present scheme and some others, where appropriate, are presented; and, numerical studies of the grid convergence and order of accuracy are also included.

The remainder of this paper is organised as follows: Sections 2 first reviews the spatial discretisation using the combined compact IRBF. Following this, Section 3 briefly describes the fully coupled approach for N-S equations. Section 4 summarises the mathematical formulation of the IBM. In Section 5, various numerical examples are presented and the present results are compared with some benchmark solutions, where appropriate. Finally, concluding remarks are given in Section 6.

2. Review of combined compact IRBF scheme

Consider a two-dimensional domain Ω, which is represented by a uniform Cartesian grid. The nodes are indexed in the x-direction by the subscript $i (i \in \{1, 2, ..., n_x\})$ and in the y-direction by $j (j \in \{1, 2, ..., n_y\})$. For rectangular domains, let N be the total number of nodes $(N = n_x \times n_y)$ and N_{ip} be the number of interior nodes $\left(N_{ip} = (n_x - 2) \times (n_y - 2)\right)$. At an interior grid point $\mathbf{x}_{i,j} = (x_{(i,j)}, y_{(i,j)})^T$ where $i \in \{2, 3, ..., n_x - 1\}$ and $j \in \{2, 3, ..., n_y - 1\}$, the associated stencils to be considered here are two local stencils: $\{x_{(i-1,j)}, x_{(i,j)}, x_{(i+1,j)}\}$ in the x-direction and $\{y_{(i,j-1)}, y_{(i,j)}, y_{(i,j+1)}\}$ in the y-direction. Hereafter, for brevity, η denotes either x or y in a generic local stencil $\{\eta_1, \eta_2, \eta_3\}$, where $\eta_1 < \eta_2 < \eta_3$, as illustrated in Fig. 1.

The integral process of the present combined compact IRBF starts with the decomposition of fourth-order derivatives of a variable, u, into RBFs;

$$\frac{d^4u(\eta)}{d\eta^4} = \sum_{i=1}^{m} w_i G_i(\eta). \tag{1}$$

Approximate representations for the third- to first-order derivatives and the functions itself are then obtained through the integration processes;

$$\frac{d^3u(\eta)}{d\eta^3} = \sum_{i=1}^{m} w_i I_{1_i}(\eta) + c_1, \tag{2}$$

$$\frac{d^2u(\eta)}{d\eta^2} = \sum_{i=1}^{m} w_i I_{2_i}(\eta) + c_1\eta + c_2, \tag{3}$$

$$\frac{du(\eta)}{d\eta} = \sum_{i=1}^{m} w_i I_{3_i}(\eta) + \frac{1}{2}c_1\eta^2 + c_2\eta + c_3, \tag{4}$$

$$u(\eta) = \sum_{i=1}^{m} w_i I_{4_i}(\eta) + \frac{1}{6}c_1\eta^3 + \frac{1}{2}c_2\eta^2 + c_3\eta + c_4, \tag{5}$$

where $I_{1_i}(\eta) = \int G_i(\eta)d\eta$; $I_{2_i}(\eta) = \int I_{1_i}(\eta)d\eta$; $I_{3_i}(\eta) = \int I_{2_i}(\eta)d\eta$; $I_{4_i}(\eta) = \int I_{3_i}(\eta)d\eta$; and, c_1, c_2, c_3, and c_4 are the constants of integration. The analytic form of the IRBFs up to eighth-order can be found in [28]. It is noted that, for the solution of second-order PDEs, only (3-5) are needed.

2.1. First-order derivative approximations

For the combined compact approximation of the first-order derivatives at interior nodes, extra information is chosen as not only $\{\frac{du_1}{d\eta}; \frac{du_3}{d\eta}\}$ but also $\{\frac{d^2u_1}{d\eta^2}; \frac{d^2u_3}{d\eta^2}\}$. We construct the conversion system over a 3-point stencil as follows.

$$\begin{bmatrix} u_1 \\ u_2 \\ u_3 \\ \frac{du_1}{d\eta} \\ \frac{du_3}{d\eta} \\ \frac{d^2u_1}{d\eta^2} \\ \frac{d^2u_3}{d\eta^2} \end{bmatrix} = \underbrace{\begin{bmatrix} \mathbf{I}_4 \\ \mathbf{I}_3 \\ \mathbf{I}_2 \end{bmatrix}}_{\mathbf{C}} \begin{bmatrix} w_1 \\ w_2 \\ w_3 \\ c_1 \\ c_2 \\ c_3 \\ c_4 \end{bmatrix}, \tag{6}$$

where $\frac{du_i}{d\eta} = \frac{du}{d\eta}(\eta_i)$ with $i \in \{1, 2, 3\}$; $\mathbf{C}$ is the conversion matrix; and, $\mathbf{I}_2$, $\mathbf{I}_3$, and $\mathbf{I}_4$ are defined as

$$\mathbf{I}_2 = \begin{bmatrix} I_{2_1}(\eta_1) & I_{2_2}(\eta_1) & I_{2_3}(\eta_1) & \eta_1 & 1 & 0 & 0 \\ I_{2_1}(\eta_3) & I_{2_2}(\eta_3) & I_{2_3}(\eta_3) & \eta_3 & 1 & 0 & 0 \end{bmatrix}. \tag{7}$$

$$\mathbf{I}_3 = \begin{bmatrix} I_{3_1}(\eta_1) & I_{3_2}(\eta_1) & I_{3_3}(\eta_1) & \frac{1}{2}\eta_1^2 & \eta_1 & 1 & 0 \\ I_{3_1}(\eta_3) & I_{3_2}(\eta_3) & I_{3_3}(\eta_3) & \frac{1}{2}\eta_3^2 & \eta_3 & 1 & 0 \end{bmatrix}. \tag{8}$$

$$\mathbf{I}_4 = \begin{bmatrix} I_{4_1}(\eta_1) & I_{4_2}(\eta_1) & I_{4_3}(\eta_1) & \frac{1}{6}\eta_1^3 & \frac{1}{2}\eta_1^2 & \eta_1 & 1 \\ I_{4_1}(\eta_2) & I_{4_2}(\eta_2) & I_{4_3}(\eta_2) & \frac{1}{6}\eta_2^3 & \frac{1}{2}\eta_2^2 & \eta_2 & 1 \\ I_{4_1}(\eta_3) & I_{4_2}(\eta_3) & I_{4_3}(\eta_3) & \frac{1}{6}\eta_3^3 & \frac{1}{2}\eta_3^2 & \eta_3 & 1 \end{bmatrix}. \tag{9}$$